

Article

The Environmental Impact of Ecological Rehabilitation Techniques Applied to Statically and Variably Stressed Welded Structures

Oana Roxana Chivu¹, Claudiu Babis^{1,*}, Augustin Semenescu¹, Olivia Doina Negoita², Gabriel Iacobescu¹ and Andrei Dimitrescu¹

- ¹ Faculty of Engineering and Management of Technological Systems, University Politehnica of Bucharest, Splaiul Independentei 313, 060042 Bucharest, Romania; virlan_oana@yahoo.co.uk (O.R.C.); asemenescu2002@yahoo.com (A.S.); gabiiacobescu@yahoo.com (G.I.); andrei_dimitrescu@yahoo.com (A.D.)
- ² Faculty of Entrepreneurship, Business Engineering and Management, University Politehnica of Bucharest, Splaiul Independentei 313, 060042 Bucharest, Romania; negoita.olivia@gmail.com
- * Correspondence: claudiubbs@gmail.com; Tel.: +40-747-270-651

Received: 12 November 2018; Accepted: 11 December 2018; Published: 14 December 2018



Abstract: There are many welded structures in the world such as bridges and viaducts that are subject to fatigue. Some of these structures, generally made of non-alloy or low-alloy steels, have been put into operation many years ago and have accumulated a large number of variable load cycles over time. For this reason, the occurrence of the fatigue phenomenon is inevitable and consists in the occurrence of failures at stresses applied to the structure, below the yield limit of the material. These stresses under the static loads would not cause the failures to appear. This paper will investigate if the ecological reconditioning techniques “weld toe grinding” and “WIG re-melting weld toe,” influence favourably the behaviour of the welded structures made from HSLA steel, in static and variable loads, if the application of these techniques is justified in both cases and finally which is the environmental impact of applying these techniques. In the paper we will present the chemical composition and mechanical properties of the base and filler materials, micro and macrostructures, graphics with the variation of the micro-hardness, we will perform static and fatigue tensile tests and we will rise the durability curve in the case of the fatigue tests. We will also present a mathematical computational algorithm, which highlights the extent to which these ecological rehabilitation techniques pollute the environment. It is more efficient both for technological and ecological reasons to recondition a product than to manufacture it from the very beginning.

Keywords: weld toe grinding; WIG re-melting weld toe; fatigue; environment; pollution; coefficient of pollution

1. Introduction

In the case of welded structures, a very large proportion is represented by fillet welded joints. Also, in the case of bridges in welded structures we often meet static loads, as well as variable loads that cause fatigue failures [1–6]. In the case of static loads, things are simpler and clearer in the sense that structural failures occur when the tear resistance of the base material is exceeded. In the case of variable loads, things are a little more complicated. In case of the welded bridges and welded structures in general, the fatigue failures are caused and can be estimated by the stress cycles accumulated over time, by the internal stress concentrators such as the type of macro-structural defects that extend over time (pore, cracks, etc.) but in the greatest extent by the external stress concentrators determined by the convex geometric shape of the welding seams [7–19]. In the past, the convex geometry of the welding seams was believed to provide better mechanical strength. In fact, this geometric shape determines

high stress concentrators at the intersection between the welding seam and the base material. The effect of these cumulative stress peaks with the variable loads to which the structures are subjected may have catastrophic effects, consisting of serious accidents that may result in loss of life. It is therefore necessary to monitor these structures and their rehabilitation in optimal conditions from a technical and economical point of view. In the case of the fatigue phenomenon, as stated before, the failure occurs at stresses below the yield strength of the base material, stresses which in the case of static loads would not even produce permanent deformations in the structure and implicitly, no failures. Variable loads are those in which there is a large number of stress cycles which is varying between a maximum and a minimum value of the stress, which as stated above is below the material yield strength. In the case of these variable loads, even if the applied loads are below the yield strength of the base material, the failure occurs due to the fact that the structure is very sensitive to the stress concentrators, which are also called “local stress peaks.” For cruciform fillet welded joints which are the subject of this work, the external stress concentrators are found at the intersection between the base and the filler material, areas named “weld toe areas” in the specialized literature and also at the root of the welding, as shown in Figure 1.

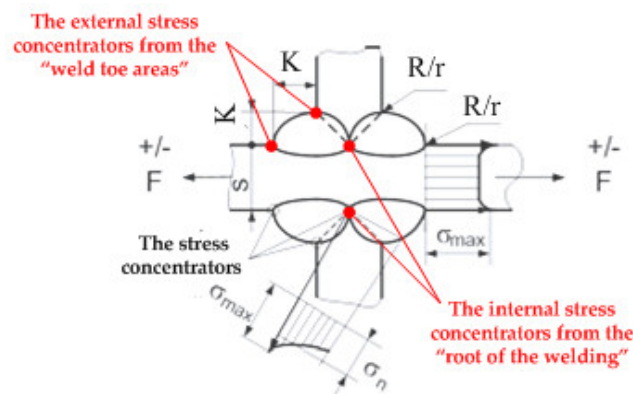


Figure 1. The “weld toe” areas, of the stress concentration; K—the cord of the welding seam; R/r the radius of the connection between the filler and the base material.

These “weld toe areas” in the case of variable loads are very dangerous and from there, many cracks are initiated that can sometimes have catastrophic effects on the structure. In Figure 1, we marked with K the cords of the welding, with R/r the radius of the connection between the filler and the base material, s is the thickness of the plates, σ_{\max} is the maximum stress, σ_n is the nominal stress and F is the force the force acting on the weld joint.

In order to ameliorate the stress peaks in the “welding toe areas” that appear as the cruciform fillet welded joints, as we have already said, we use several ecological rehabilitation techniques. These techniques aim to increase the connection radius between the base and the filler material, in order to reduce the stress concentration. In this paper we will analyse the effects of the influence of those two rehabilitation techniques: the “grinding weld toe” rehabilitation technique and the “WIG re-melting weld toe” rehabilitation technique [20–22]. The “grinding weld toe” rehabilitation technique consists in the milling of the top of the welding cord, along the intersection line between the filler and the base material, for the joints between the pipes (T, Y or K) and for the fillet weld joints between the tables. The tools recommended for this process are the wolfram high-speed finger cutters. The “WIG re-melting weld toe” rehabilitation technique consists of re-melting the weld metal to a depth of about 2 mm across the welding toe, without adding a filler material.

In this paper a comparison is made between the effects of those two mentioned rehabilitation techniques applied on the cruciform fillet welded joints, both in the case of static and variable loads, in order to draw conclusions about the efficiency of these techniques depending on the type of load.

Also, the ecological impact on the environment after applying these rehabilitation techniques is studied [23–26].

2. Materials and Methods

The object of the study presented in this paper is the cruciform fillet welded sample marked with D. The cruciform fillet welded sample marked with D, as we can see from Figure 2 is made from two vertical plates and a horizontal one, all welded by using the shielded gas welding procedure, with full wire and three welded rows in horizontal position. The cruciform fillet welded sample marked with D is shown as shape and dimensions in Figure 2. The dimensions of the cruciform fillet welded sample marked with D, presented in Figure 2, are expressed in millimetres.

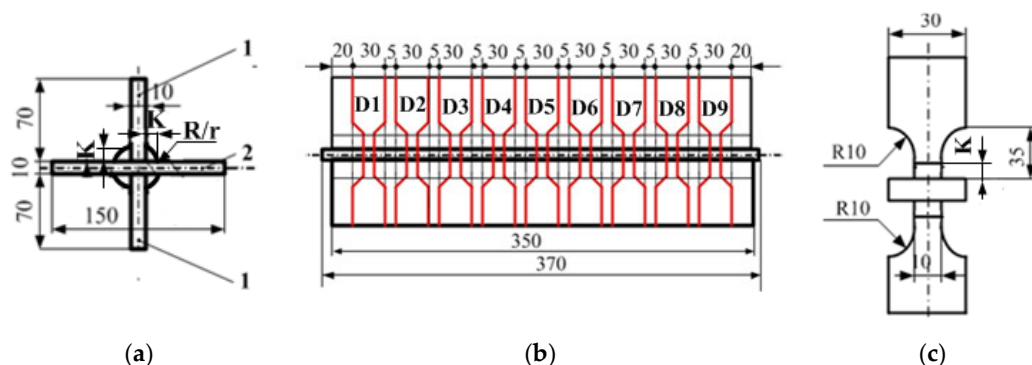


Figure 2. The shape and size of the welding sample D, expressed in millimetres; (a) front view sketch welding sample, (b) test specimens from D1–D9, (c) static and fatigue specimen tests after milling.

The material from which the cruciform fillet welded sample D is made is a high-strength low-alloy steel (HSLA). This material is a type of steel alloy that provides better mechanical properties or greater resistance to corrosion than carbon steel. HSLA steels vary from other steels in that they are not made to meet a specific chemical composition but rather specific mechanical properties. They have a carbon content between 0.05–0.25% to retain formability and weldability. Other alloying elements include up to 2.0% manganese and small quantities of copper, nickel, niobium, nitrogen, vanadium, chromium, molybdenum, titanium, calcium, rare earth elements, or zirconium. Copper, titanium, vanadium and niobium are added for strengthening purposes. These elements are intended to alter the microstructure of carbon steels, which are usually a ferrite-pearlite aggregate, to produce a very fine dispersion of alloy carbides in an almost pure ferrite matrix. This eliminates the toughness-reducing effect of a pearlite volume fraction yet maintains and increases the material's strength by refining the grain size, which in the case of ferrite increases yield strength by 50% for every halving of the mean grain diameter. Precipitation strengthening plays a minor role, too. Their yield strengths can be anywhere between 250–590 megapascals (36,000–86,000 psi). Because of their higher strength and toughness HSLA steels usually require 25 to 30% more power to form, as compared to carbon steels.

Copper, silicon, nickel, chromium and phosphorus are added to increase corrosion resistance. Zirconium, calcium and rare earth elements are added for the sulphide-inclusion shape control which increases formability. These are needed because most HSLA steels have directionally sensitive properties. Formability and impact strength can vary significantly when tested longitudinally and transversely to the grain. Bends that are parallel to the longitudinal grain are more likely to crack around the outer edge because it experiences tensile loads. This directional characteristic is substantially reduced in HSLA steels that have been treated for the sulphide shape control.

HSLA are used in cars, trucks, cranes, bridges, roller coasters and other structures that are designed to handle large amounts of stress or need a good strength-to-weight ratio. HSLA steel cross-sections and structures are usually 20 to 30% lighter than a carbon steel with the same strength.

HSLA steels are also more resistant to rust than most carbon steels because of their lack of pearlite—the fine layers of ferrite (almost pure iron) and cementite in pearlite. HSLA steels usually have densities of around 7800 kg/m³.

The chemical composition for the 945 A HSLA steel is presented in Table 1.

Table 1. The chemical composition for the 945 A HSLA steel.

Grade	C-max (%)	Mn-max (%)	P-max (%)	S-max (%)	Si-max (%)	Notes
945A	0.15	1.0	0.04	0.05	0.9	-

The mechanical properties for the 945 A HSLA steel are presented in Table 2.

Table 2. The mechanical properties for the 945 A HSLA steel.

Grade	Form	Yield Strength-min (MPa)	Ultimate Tensile Strength-min (MPa)
945A	Plates, shapes and bars	310	448

Nine specimens marked with D1-D9 were cut from welding sample D, as we can see in Figure 2b. The specimens marked with D1, D4 and D7 have been used for static traction tests until fracture, the other specimens marked with D2, D3, D5, D6, D8 and D9 have been used for fatigue tests. Those two rehabilitation techniques, the “welding toe grinding” and “WIG re-melting welding toe” were applied before static and fatigue tests were carried out, as follows: D2 and D3 are specimens with no rehabilitation techniques applied, D5 and D6 are specimens on which the “grinding weld toe” rehabilitation technique is applied and D8 and D9 are the specimens with the “WIG re-melting welding toe” rehabilitation technique applied. Both the static and fatigue specimens were obtained by the mechanical cutting from the cruciform fillet welded sample D of the strips with 30 mm widths, as seen in Figure 2b. After the mechanical cutting, the vertical plates of the joint will be milled to reduce the width in the welded area from 30 to 10 mm, as shown in Figure 2c. The reducing of the cross-section was done in order to guide both the static traction and the fatigue fracture in the area of the welding seam or its heat affected zone HAZ. It is noticed that the cross section is not reduced sharply from 30 to 20 mm and milling is done with a radius connection R = 10 mm, in order not to introduce additional stress concentrators.

The filler material used for the GMAW welding procedure of the welding sample D is ER 70S-3in accordance with the specifications of ANSI/AWS A5.18. Yielding almost a slag free quality weld deposit on most steels provides an excellent welder satisfaction for post weld clean up. Some typical application includes structural steel, steel buildings, auto frames, sheet metal, ships, barges, railcars, trailers, ornamental iron, furniture storage bins, earthmoving and farm equipment.

The welding parameters for our application using GMAW procedures with spray arc regime is presented in Table 3. We used for gas protection, 100% CO₂.

Table 3. The welding parameters for GMAW procedures.

Wire Diameter (mm)	Wire Speed (m/min)	Amperes	Volts	Travel Speed (m/min)	Flow Gas Protection (L/min)
1.2	4.3	235–240	22–23	3.04	14–16

The welding regime parameters used for welding the sample marked with D are presented in Table 3, where I_s is the intensity of the welding current, U_a is the voltage, t_s is the welding time, L_c is the seam length, V_s is the welding speed, V_{as} is the wire feed speed and E_l is the linear energy.

Typical wire chemistry is presented in Table 4, the weld metal properties are shown in Table 5, the CO₂ emissions resulted after welding depending on the welding process used are presented, in Table 6.

Table 4. Typical wire chemistry.

	AWS Specifications	Typical Wire 70S3
C (%)	0.060–0.15	0.10
Mn (%)	0.90–1.40	1.00
Si (%)	0.45–0.75	0.55
P-max (%)	0.025	0.012
S-max (%)	0.035	0.012

Table 5. The weld metal properties.

Properties	AWS Specifications	Typical Wire 70S3
Tensile Strength (MPa)	0.482	0.517
Yield Strength (MPa)	0.399	0.430
Elongation—min (%)	22	30.7
Charpy-V notch at 0 °C (J)	27.12	81.35
Reduction of area (%)	n/a	59
Average Brinell Hardness (Brinell units)	n/a	130

Table 6. CO₂ emissions when welding.

Welding Process	CO ₂ Emissions (Tons of CO ₂ /Tons of Welded Seam)	
	Minimum	Maximum
Manual with electric arc and coated electrode	0.280	0.50
Automated with submerged arc flux	0.175	0.21
In shielded gas environment	0.205	0.24
By the oxy-gas flame	0.312	0.55

For the fatigue and tensile tests, we used the LVF 100-FM machine, with the following technical features: maximum static load + /− 100 KN; maximum dynamic load + /− 100 KN; maximum working frequency 50 Hz; piston stroke 100 mm; distance between gripping devices 1200 mm; overall dimensions WxDxH 900 × 600 × 2510 mm; weight about 830 Kg; pump flow 44 L/min/200 bar.

The fatigue tests are made according to the data of the experimental plan presented in Table 7.

Table 7. Fatigue tests.

No.	Rehabilitation Technique	Sample Mark	Frequency (Hz)	Force + /− Fi (kN)
1	Without rehabilitation	D2	10	±14
2		D3		±7.5
3	Grinding weld toe	D5		±14
4		D6		±7.5
5	WIG re-melting weld toe	D8		±14
6		D9		±7.5

In the case of the technological process of manufacturing the structural elements that make up the bridge, we must also take into account the pollution introduced into the environment when elaborating the basic materials from which the structural elements of the bridge are made. The emissions and the polluting products result from the elaboration of a ton of steel are shown in Table 8. These data were taken from the literature [27].

Table 8. Emissions and pollutants produced when elaborating a ton of steel.

No.	Emission or Sub Product	Measurement Unit	Amount (Max.)
1	Dust in the air	Kg/t steel	0.64
2	CO	Kg/t steel	28
3	SO ₂	Kg/t steel	1.83
4	NO _x	Kg/t steel	1.35
5	CO ₂	Kg/t steel	2040
6	Flue gases(others)	Kg/t steel	23.000
7	Slag	Kg/t steel	455
8	Mud	Kg/t steel	58
9	Dust deposited	Kg/t steel	30
10	Other deposits	Kg/t steel	8
11	Refractory subproducts	Kg/t steel	4
12	Used water	Kg/t steel	20
13	Oils	Kg/t steel	0.8
TOTAL		Kg/t steel	25.650

The material from which the product is made is the most important element in terms of the environmental impact because the material preparation is the most polluting stage in the technological path of a product. Therefore, in order to make it possible to calculate the coefficient of pollution introduced at this stage, we have to take into account more knowledge.

Besides the mechanical resistance characteristics, the material must also exhibit very good resistance against external chemical agents, different in nature, concentration and way of interacting with the metal.

Next, the methodology for calculating the coefficients of pollution for each stage of the technological process of manufacturing the bridge in welded constructions, the total coefficient of pollution and the calculation of the environmental quality indicator are presented below. The formula is taken from the literature [27]. It goes without saying that in the eco-technological process of reconditioning many of the stages of the manufacturing process will be missing. In these missing stages, the stage coefficients of pollution will be null.

*The coefficient of pollution introduced by the semi-finished product C_{ps} expressed in tons of emissions, can be calculated by relation 1, knowing the useful mass of the semi-finished product used to make the product.

$$C_{ps} = Q_{ts} \cdot M_{su} = (Q_{sa} + Q_{sl} + Q_{ss}) \cdot M_{su} \quad (1)$$

where Q_{ts} is the total amount of pollutant introduced by the semi-finished product expressed in tons of emissions/ton of useful semi-finished product; Q_{sa} is the amount of substance that pollutes the air during the elaboration of the semi-finished product; Q_{sl} is the amount of substance polluting the water in the elaboration of the semi-finished product; Q_{ss} is the amount of substance polluting the soil in the elaboration of the semi-finished product and M_{su} is the useful mass of the semi-finished product, in tons.

Also, in the material and semi-finished product elaboration stage there is an acute pollution of the waters by the metallurgical pollutants present in the aqueous environment circumscribed to the technological contour. The most important pollutants are fog, aerosols and smog formation.

The coefficient of pollution introduced when supplying with raw materials C_{pa} , expressed in tons of emissions can be calculated by relation 2, where Q_{pa} is the amount of materials polluting the atmosphere and Q_{ps} is the amount of materials polluting the soil.

$$C_{pa} = Q_{pa} + Q_{ps} \quad (2)$$

Air pollution and soil pollution are caused by NO_x and various types of oils, greases and even fuels eliminated by the trucks that supply the raw materials. All the primary energy materials used for

combustion contain carbon in the form of chemical combinations, which oxidize transforming into carbonic gas (CO₂) or carbon oxide (CO) if the combustion is incomplete.

The distance travelled by the trucks to supply the raw material to the enterprise where the product is made is of 50 km.

The coefficient of pollution introduced for cleaning, pickling, degreasing C_{pcd} , expressed in tons of emissions, can be calculated by relation 3 in which Q_{ptc} is the total amount of the polluting substance in the cleaning, pickling, degreasing operation, Q_{pca} is the amount of the atmosphere pollutant which appears in the cleaning, pickling, degreasing and M_u represents the useful mass of the semi-finished-product or the semi-finished-piece.

$$C_{pcd} = Q_{ptc} \cdot M_u = Q_{pca} \cdot M_u \quad (3)$$

The coefficient of pollution introduced by the mechanical processing C_{pm} , expressed in tons of emissions, is calculated by the relation 4, where Q_{tmp} is the total amount of polluting substance occurring in the mechanical processing, in tons of emissions/tons of product, Q_{pma} the amount of substance polluting the air that occurs in the mechanical processing, in tons of emissions/tons of product, Q_{pml} the amount of substance polluting the water that occurs in mechanical processing, in tons of emissions/tons of product, Q_{pms} the amount of substance polluting the soil occurring in the mechanical processing in tons of emissions/tons of product and M_u the amount of useful substance used to make the product, in tons.

$$C_{pm} = Q_{tmp} \cdot M_u = (Q_{pma} + Q_{pml} + Q_{pms}) \cdot M_u \quad (4)$$

The coefficient of pollution introduced by the products control and inspection noted with C_{cp} , expressed in Kilograms of emissions, can be calculated by relation 5 where Q_{cp} is the total amount of polluting substance occurring during the control or inspection operations, Q_{pca} the amount of substance polluting the air that occurs during the control or inspection process, Q_{pcl} the amount of substance polluting the water that occurs in the control or inspection process, Q_{pcs} the amount of substance polluting the soil occurring during the control or inspection operations and M_u is the mass of the controlled substance in kg.

$$C_{cp} = Q_{cp} \cdot M_u = (Q_{pca} + Q_{pcl} + Q_{pcs}) \cdot M_u \quad (5)$$

The coefficient of pollution introduced for recovery, recycling and reconditioning noted with C_{pr} , can be calculated by relation 6 where Q_{tp} is the total amount of polluting substance, expressed in emissions, kg of reconditioned, recycled substance, Q_{pra} the amount of substance polluting the air during the repair, reconditioning, recycling operations, in kg emissions/kg, Q_{prl} the amount of substance polluting the water during the repair, reconditioning, recycling operations, in kg emissions/kg, Q_{prs} the amount of substance polluting the soil during the repair, reconditioning, recycling operations, in kg emissions/kg, N_{pr} number of repaired, reconditioned, recycled products and M_{ur} is the useful material mass, resulted after repair, reconditioning, recycling, expressed in kg.

$$C_{pr} = Q_{tp} \cdot M_{ur} = (Q_{pra} + Q_{prl} + Q_{prs}) \cdot N_{pr} \quad (6)$$

The other stages in the flow diagram of the technological process of making a product have a lower impact on the environment, some of them even having zero impact. Therefore, in order to capture their impact on environmental pollution as efficiently and conclusively as possible, we can have for the C_{pax} auxiliary coefficient of pollution, expressed in kilograms of emissions, the value given by expression (7), where C_{pe} is the coefficient of pollution introduced in the elaboration of the material from which the product is made.

$$C_{pax} = C_{pe} \cdot (0.001..0.01) \quad (7)$$

Knowing the coefficients of pollution introduced at each stage of the technological process of making the product, we can determine the total coefficient of pollution C_{pt} , expressed in kilograms of emissions by relation 8, where C_{pa} is the coefficient of pollution introduced by the supply operation, C_{ps} the coefficient of pollution introduced in the elaboration of the semi-finished product, C_{pcd} the coefficient of pollution introduced by the cleaning, pickling and degreasing operation, C_{pm} the coefficient of pollution introduced by the mechanical processing, C_{pr} the coefficient of pollution introduced by the recovery, recycling, reconditioning, C_{cp} the coefficient of pollution introduced by the product's control (inspection) and C_{pax} the coefficient of pollution introduced by the other stages of the flow diagram of the technological process.

$$C_{pt} = C_{ps} + C_{pa} + C_{pcd} + C_{pm} + C_{cp} + C_{pr} + C_{pax} \quad (8)$$

A correct design of a technological process or activity with an environmental impact requires the knowledge of the I_{cm} environmental quality indicator at each stage. This indicator can be calculated at the level of each pollutant i , by relation 9, where I_{cmi} is the environmental quality indicator due to the pollutant "i", CMA_i is the maximum allowable concentration in the pollutant "i", C_{efi} is the effective concentration, at the time of the calculation, in the pollutant "i" and C_{maxi} the maximum concentration in the pollutant "i" leading to the unavoidable degradation of the environment.

$$I_{cmi} = CMA_i - C_{efi}/C_{maxi} - CMA_i \quad (9)$$

The environmental quality indicator due to all the pollutants "p" in the environment at the time of the calculation is noted with I_{cmt} and is calculated by relation 10.

$$I_{cmt} = \sum_{i=1}^P (CMA_i - C_{efi}/C_{maxi} - CMA_i) \quad (10)$$

The environmental indicators for certain elements with normal values, alert thresholds and intervention thresholds are shown in Table 9.

Table 9. Environmental indicators for certain chemical elements.

Indicators	Normal Values (mg/kg Dry Substance)	Alert Thresholds (mg/kg Dry Substance)	Intervention Thresholds (mg/kg Dry Substance)
Cadmium	1	5	10
Chromium	30	300	600
Copper	20	250	500
Zinc	100	700	1500
Lead	20	250	1000
Nickel	20	200	500
Manganese	900	2000	4000

3. Results and Discussion

In Figure 3, we show schematically the cross sections of the specimens, obtained from samples D, after applying the rehabilitation techniques. The dimensions of the cross sections from Figure 3 are expressed in millimetres.

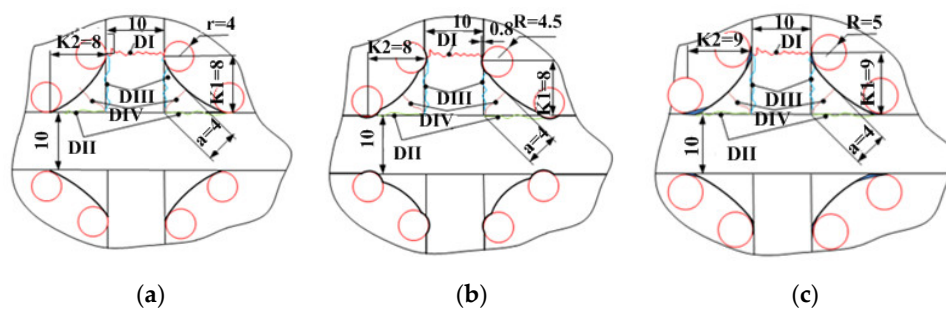


Figure 3. The cross sections of the specimens: (a) Specimens D1, D2, D3 without rehabilitation; (b) Specimens D4, D5, D6 by using the “grinding weld toe” rehabilitation technique; (c) Specimens D7, D8, D9 by using the “WIG re-melting weld toe” rehabilitation technique.

Figure 3a shows that in the case of specimens D1, D2 and D3 without the applied rehabilitation technique, the welding cords are 8 mm in size, the thickness of the welding seam have a value of 4 mm and the connecting rays between the filler and the base material marked with r/R have the value of 4 mm.

Figure 3b shows that in the case of specimens D4, D5 and D6 using the “grinding weld toe” rehabilitation technique, the welding cords are 8 mm in size, the thickness of the welding seam have a value of 4 mm and the connecting rays between the filler and the base material marked with r/R have the value of 4.5 mm.

Figure 3c shows that in the case of specimens D7, D8 and D9 using the “WIG re-melting weld toe” rehabilitation technique, the welding cords are 9 mm in size, the thickness of the welding seam have a value of 4 mm and the connecting rays between the filler and the base material marked with r/R have the value of 5 mm.

The geometric elements K1, K2 and R/r of the welding seams of the specimens from samples D, are shown in Table 10, where a is the aperture of the welding seam, K1 and K2 are the seam legs and R/r is the radius between the seam and the base material.

Table 10. Geometric elements of the welding seams for specimen sample D.

Specimen	a (mm)	K1 = K2 (mm)	r/R (mm)
D1, D2 and D3	4	8	4
D4, D5 and D6	4	8	4.5
D7, D8 and D9	4	9	5

These geometric elements were determined by measurements made by means of a specialized software in the macroscopic analysis presented in Figure 4. The macroscopic analysis was performed for each specimen used for the static tensile tests as follows: specimen D1 without rehabilitation, specimen D4 on which we apply the “grinding weld toe” rehabilitation technique and specimen D7 by using the “WIG re-melting weld toe” rehabilitation techniques. The dimensions of the cross sections for specimens D1; D4 and D7 are expressed in millimetres.

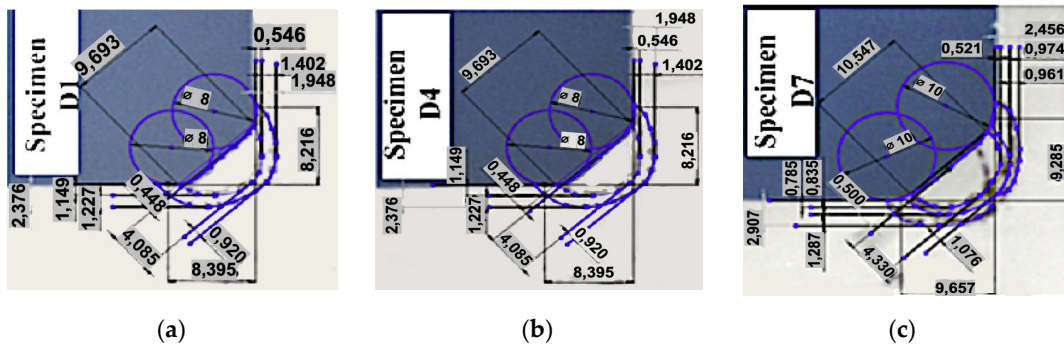


Figure 4. The macroscopic analysis: (a) For the specimen D1 without rehabilitation; (b) For specimen D4 by using the “grinding weld toe”; (c) For specimen D7 by using the “WIG re-melting weld toe.”

Also, the microscopic analysis for the same specimens for the most important areas of the welding such as: the base material marked with BM, the filler material marked with FM and the heat affected zone marked with HAZ is presented in Figure 5. The microscopic analysis is made according to EN-1321/200 at 500X magnification factor. The metallographic analysis did not reveal structures outside the equilibrium.

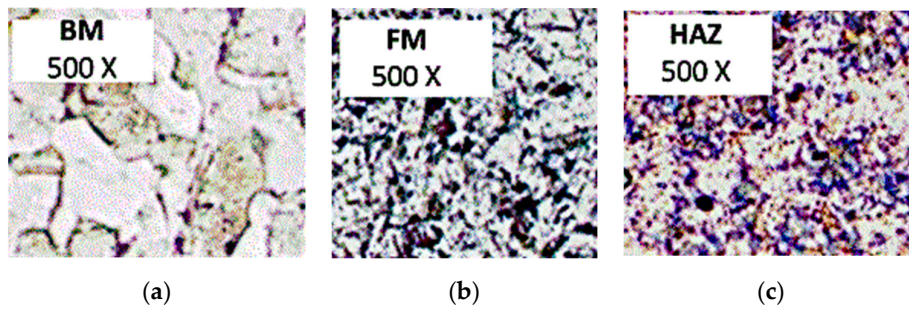


Figure 5. The microscopic analysis: (a) For specimen D1 without rehabilitation; (b) For the specimen D4 using the “grinding weld toe”; (c) For specimen D7 using the “WIG re-melting weld toe.”

The measurements for micro-hardness HV 0,1 are made according to EN 9015-2-2016 along the axes I and II, as we can see from Figure 6 and the variation of micro-hardness from the axes I and II is shown in Figure 7.

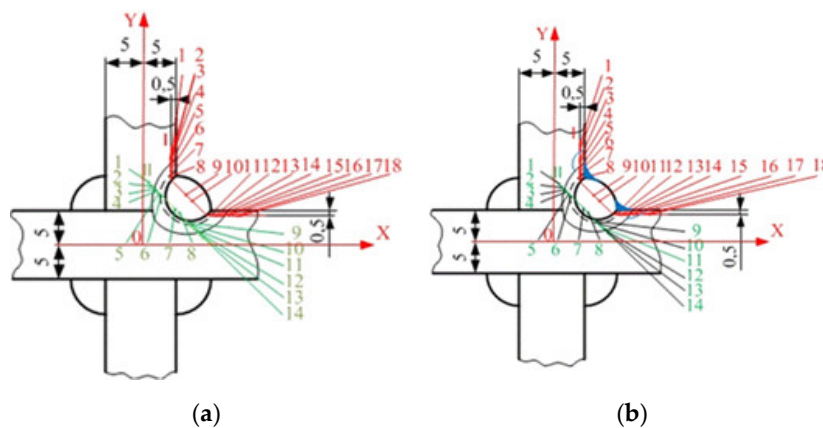


Figure 6. The measurements for micro-hardness HV 0.1: (a) For specimens D1 without rehabilitation and for D4 using the “grinding weld toe”; (b) For the specimen D7 using the “WIG re-melting weld toe.”

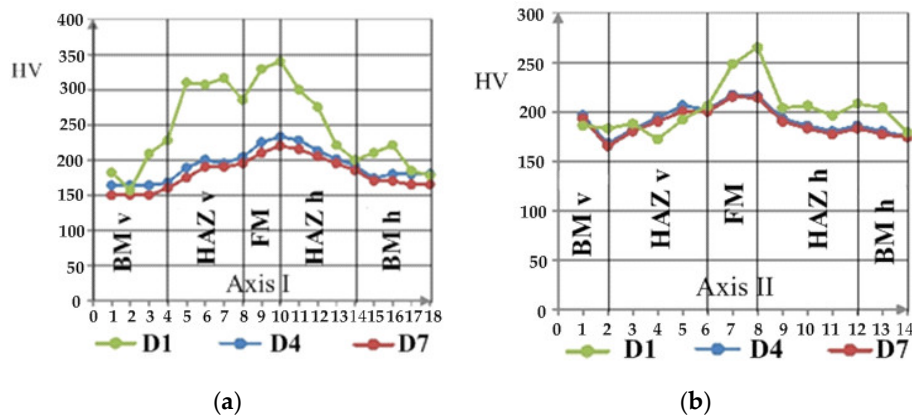


Figure 7. The variation of micro-hardness HV 0.1: (a) For specimens D1, D4 and D7 from axis I; (b) For specimens D1, D4 and D7 from the axis II.

The measurements of micro-hardness are made by the method of finger printing in rows on two perpendicular directions along the plate (horizontal and vertical direction-axis I) and a diagonal direction oriented at 120° to the horizontal sheet plane (axis II), which should contain the root of the welding seam, as shown in Figure 6a for specimens D1 and D4 and in Figure 6b for the specimen D7.

We can observe that the lowest value of the micro-hardness is obtained in the case of specimen D7 by using the “WIG re-melting weld toe” rehabilitation techniques and the highest for specimen D1 without any rehabilitation techniques applied.

The static tensile tests until failure, for D1, D4 and D7 specimens are presented in Figure 8. The fatigue test specimens for samples D, one from each set, caught in the test machine’s jets, are presented in Figure 9.

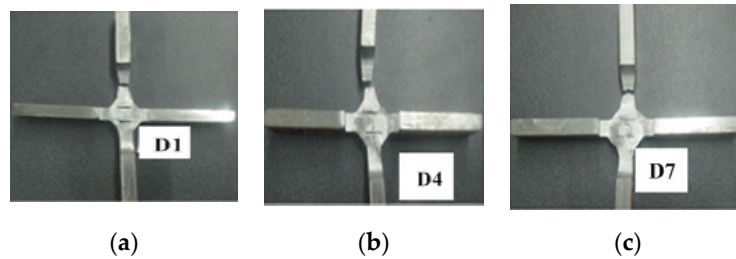


Figure 8. The static tensile tests: (a) For specimen D1 without rehabilitation; (b) For specimen D4 by using the “grinding weld toe”; (c) For specimen D7 by using the “WIG re-melting weld toe.”

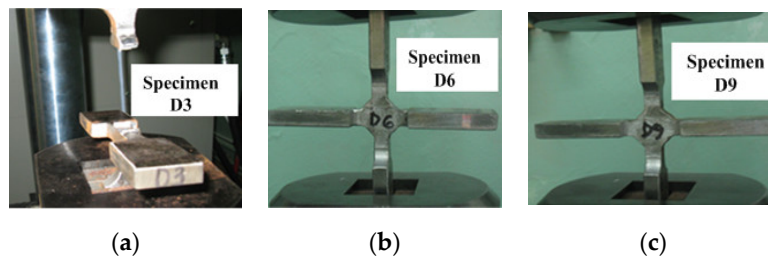


Figure 9. Fatigue tests: (a) For specimen D3 without rehabilitation; (b) For specimen D6 by using the “grinding weld toe”; (c) For specimen D9 by using the “WIG re-melting weld toe.”

The stress strain curves plotted by the machine software for the static tensile tests’ specimens are presented in Figure 10. We can observe that from specimens made from an HSLA steel, in the case of the static loads, the rehabilitation technique does not influence the value of the tensile strength.

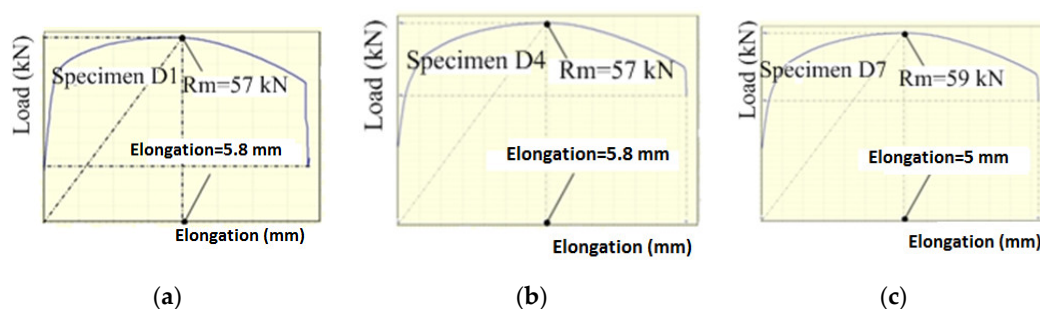


Figure 10. The stress-strain curves for the static tensile tests: (a) For specimen D1 without rehabilitation; (b) For specimen D4 by using the “grinding weld toe”; (c) For specimen D7 by using the “WIG re-melting weld toe.”

All the fatigue tests were performed at the 10 Hz frequency, the stress cycle being a symmetrical alternating one, with the asymmetry coefficient $R = -1$, the cycle stress being that of the tension compression one. For the three sets of fatigue specimens for sample D, with and without reconditioning techniques applied, three durability curves were drawn and then compared. For tracing the durability curves, two variations of the force were applied to the fatigue test specimens of sample D (and the third between them was interpolated), as follows: for the first set of specimens without rehabilitation we apply to $D2 \pm 14$ kN, to $D3 \pm 7.5$ kN, for the second set of the specimens with “grinding weld toe” rehabilitation techniques we apply for $D5 \pm 14$ kN, for $D6 \pm 7.5$ kN and for the third set of test specimens by using the “WIG re-melting weld toe” rehabilitation techniques, we apply to $D8 \pm 14$ kN and to $D9 \pm 7.5$ kN. The forces applied to the specimens for sample D and the results obtained from the fatigue tests are presented and centralized in Table 11.

Table 11. Results from the fatigue tests for specimens for sample D.

No.	Rehabilitation Technique	Mark	Frequency (Hz)	Force + / - F_i (kN)	Time(s)	Number of Cycles Until Failure ($N = t \cdot f$)
1	Without rehabilitation	D2	10	± 14	1850	18.500
2		D3		± 7.5	22.890	228.900
3	Grinding weld toe	D5		± 14	2682	26.820
4		D6		± 7.5	33.189	331.890
5	WIG re-melting weld toe	D8		± 14	5457	54.570
6		D9		± 7.5	68.672	686.720

The traceability of the durability curves presented in Figure 11, is based on the law of variation of the durability curve in linear coordinates, given by expression (11).

$$\Delta\sigma(n) = \sqrt[p]{\frac{10^r}{n}} \quad (11)$$

in expression (11) where $\Delta\sigma$ is the stress variation, $1/p$ is the slope of the curve, $r = \lg A$ is the intersection between the curve and vertical axis and n is number of cycles.

For sample D, using the Mathcad calculation program, for specimens D2, D3, with no rehabilitation technique, we found the values $p = 2$ and $r = 6.7$, for which the graph of the function $\sigma_{1d}(n)$ approaches most of our points $d1 = (18,500; 46,128; 228,904)$ and which represents the force vector $f = (14; 9; 6)$. The shape of this curve is shown in Figure 11, with green dot line. For the second set of specimens D5, D6 by using the “weld toe grinding,” also with the help of Mathcad, the values $p = 2$ and $r = 6.8$ were found for which the graph of the function $\sigma_{2d}(n)$ is closer to our points our $d2 = (26,820; 179,358; 331,896)$ and the force vector is $f = (14; 9; 6)$. The shape of this curve is also shown in Figure 11, with the broken green line. For the third set of specimens D8, D9 by using the “WIG

re-melting weld toe,” also employing the Mathcad program, we found the values $p = 2$ and $r = 7.2$ for which the graph of the function $\sigma_{3d}(n)$ approaches one of our points $d_3 = (54,570; 370,645; 686,720)$ and the force vector is $f = (14; 9; 6)$. The shape of this curve is also shown in Figure 11 with green continue line.

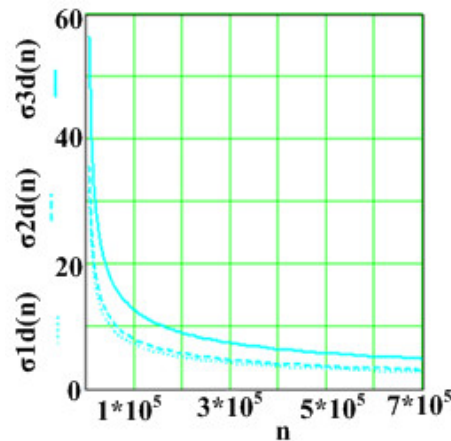


Figure 11. The durability curves: n -number of cycles, $\sigma_{1d}(n)$, $\sigma_{2d}(n)$, $\sigma_{3d}(n)$ -the mathematical functions of the durability curves.

We can see from Table 11 and Figure 11 that in the case of the welded structure made from an HSLA steel, that the longest fatigue life time is achieved by using the “WIG re-melting weld toe” technique and the smallest if no rehabilitation technique is applied. The explanation is that by applying the rehabilitation techniques the stress concentrators are removed from the intersection between the base and the filler material, obtaining a smooth connection between them. The biggest smooth connection and the longest fatigue life time is achieved with applying the “WIG re-melting weld toe” technique.

From the point of view of the environmental impact the application results of the technological process of manufacturing the bridges in the welded construction as well as of the rehabilitation technologies “weld toe grinding” and “WIG re-melting weld toe,” are presented below. The results were determined by the calculation algorithm presented at point 2 of the paper. For the calculation of the total coefficient of pollution, the coefficients for each stage of the eco-technological production process must be calculated. In this regard, their calculation in numerical form is presented below.

First, for the bridge welding manufacturing, we have the following results.

The coefficient of pollution introduced by the semi-finished product C_{ps} expressed in tons of emissions.

According to the data in Table 8, the calculation of the amounts of substances that pollute the air, water and soil consists of the following.

Regarding the air pollution we have air dust = 0.64 kg/t steel; CO = 28 kg/t steel; SO₂ = 1.83 kg/t steel; NO_x = 1.35 kg/t steel; CO₂ = 2040 kg/t steel; Flue gases (others) = 23,000 kg/t steel. Total $Q_{sat} = 0.64 + 28 + 1.83 + 1.35 + 2040 + 23,000 = 25,071$ kg/t steel.

The main substances polluting the water areas follows Mud = 58 kg/t steel, Used water = 20 kg/t steel and Oils = 0.8 kg/t steel. Total $Q_{slt} = 58 + 20 + 0.8 = 78.8$ kg/t steel.

The substances contributing to the soil pollution areas follows Slag = 455 kg/t steel, Dust deposited = 30 kg/t steel, Refractory sub-products = 4 kg/t steel, Other deposits = 8 kg/t steel. Total $Q_{sst} = 455 + 30 + 4 + 8 = 497$ kg/t steel.

Consequently $C_{ps} = (25.071 + 0.0788 + 0.497) \cdot 0.5 = 12.82$ tons of emissions.

The coefficient of pollution introduced when supplying with raw materials C_{pa} .

The distance travelled by the trucks to supply raw material to the enterprise where the “Condensation Tank” product is made is of 50 km.

The air pollution when supplying with raw materials consists of $\text{CO}_2 = 150 \text{ g/km}$ and $\text{CO} = 100 \text{ g/km}$. Consequently $Q_{pa} = 150 \text{ g CO}_2 \cdot 50 = 7500 \text{ g}$ and $Q_{pa} = 100 \text{ g CO} \cdot 50 = 5000 \text{ g}$ where Q_{pa} is the materials amount polluting the atmosphere.

The soil pollution consists of Benzene = 0.01 mg/km (dry substance), from which we have $Q_{ps} = 0.01 \text{ mg} \cdot 50 = 0.0005 \text{ g}$ where Q_{ps} is the materials amount polluting the soil. In total $C_{pa} = Q_{pa} + Q_{ps} = 7500 \text{ g} + 5000 \text{ g} + 0.0005 \text{ g} = 12,500 \text{ g} = 12.5 \text{ kg}$, where C_{pa} is the coefficient of pollution when supplying.

The coefficient of pollution introduced in the cleaning, pickling and degreasing C_{pcd}

In the cleaning, pickling and degreasing operations there will be emissions of volatile substances in the atmosphere of 0.001 t/kg . Consequently, $C_{pcd} = Q_{ptc} \cdot M_u = Q_{pca} \cdot M_u$ (kg emissions) = $0.001 \cdot 0.5 = 0.0005 \text{ kg emissions}$, where Q_{ptc} is the total amount of the polluting substance, which occurs in the cleaning, pickling, degreasing, Q_{pca} is the total amount of the substance polluting the atmosphere which occurs in the cleaning, pickling, degreasing and M_u is the useful mass of the semi-finished product or semi-finished piece.

The coefficient of pollution introduced by the mechanical processing C_{pm}

For the case, the material removed by cutting/splintering is to be calculated, knowing the weight of the semi-finished product and the product. The coefficient of pollution introduced by the mechanical processing C_{pm} given by relation $C_{pm} = Q_{tmp} \cdot M_u = (Q_{pma} + Q_{pml} + Q_{pms}) \cdot M_u$ where Q_{tmp} is the total amount of polluting substance occurring in the mechanical processing in tons of emissions/tons of product, Q_{pma} is the amount of substance polluting the air that occurs in the mechanical processing in tons of emissions/tons of product, Q_{pml} is the amount of substance polluting the water that occurs in the mechanical processing in tons of emissions/tons of product, Q_{pms} is the amount of soil polluting substance occurring in the mechanical processing in tons of emissions/tons of product and M_u is the amount of useful substance used to make the product in tons. $C_{pm} = 0.001 \times 0.5 = 0.0005 \text{ tons of emissions}$.

The coefficient of pollution introduced by the products' control and inspection noted with C_{cp} .

The volatile organic compounds and aerosols resulting from the penetrating fluid control are dangerous to both eyes and breathing. To see the environmental impact introduced by the control or inspection operations, we calculate the total coefficient of pollution C_{pc} , using an expression of the type $C_{cp} = Q_{pt} \cdot M_u = (Q_{pca} + Q_{pcl} + O_{pcs}) \cdot M_u$ expressed in kg of emissions, where Q_{cp} is the total amount of polluting substance occurring during the control or inspection operations, Q_{pca} is the amount of substance polluting the air that occurs during the control or inspection process, Q_{pcl} is the amount of substance polluting the water that occurs in the control or inspection process, O_{pcs} is the amount of soil polluting substance occurring during the control or inspection operations and M_u is the mass of the controlled substance, in kg. Consequently, by considering $Q_{pt} = 0.030 \text{ kg/ton of steel}$ we have $C_{cp} = 0.030 \cdot 0.5 = 0.015 \text{ kg of emissions}$.

The coefficient of pollution introduced for recovery, recycling and reconditioning noted with C_{pr} .

This coefficient is neglected for our product.

The Auxiliary coefficient of pollution C_{pax} .

The other stages in the flow diagram of the technological process of making a product have a lower impact on the environment, some of them even have zero impact. Therefore, in order to capture their impact on the environmental pollution as efficiently and conclusively as possible, we can have for the C_{pax} auxiliary coefficient of pollution, the value given by the expression $C_{pax} = C_{pe} \cdot (0.001 - 0.01)$ expressed in kg of emissions, where C_{pe} is the coefficient of pollution introduced in the elaboration of the material from which the product is made and has the value of $25.65 \text{ kg of emissions}$. We have as result $C_{pax} = 25.65 \cdot 0.01 \text{ kg of emissions} = 0.2565 \text{ kg of emissions}$.

The Total coefficient of pollution C_{pt} .

Knowing the pollution coefficients introduced at each stage of the technological process of making the product we can determine the total coefficient of pollution C_{pt} , expressed in kilograms of emissions by the relation $C_{pt} = C_{ps} + C_{pa} + C_{pcd} + C_{pm} + C_{cp} + C_{pr} + C_{pax}$ where C_{pa} is the coefficient of pollution introduced by the supply operation, C_{ps} is the coefficient of pollution introduced in the elaboration

of the semi-finished product, C_{pcd} is the coefficient of pollution introduced by the cleaning, pickling and degreasing operation, C_{pm} the coefficient of pollution introduced by the mechanical processing, C_{prrr} the coefficient of pollution introduced by the recovery, recycling, reconditioning and C_{pax} the coefficient of pollution introduced by the other stages of the flow diagram of the technological process. We obtain as result $C_{pt} = 12,820 \text{ kg} + 12.5 \text{ kg} + 0.0005 \text{ kg} + 0.5 \text{ kg} + 0.015 \text{ kg} + 0 + 0.256 \text{ kg} = 12.833 \text{ t}$.

Second, for applying the “weld toe grinding” technique, we have the following results.

*The coefficient of pollution introduced by the semi-finished product C_{ps} is zero.

*The coefficient of pollution introduced by the raw material supply C_{pa} is also zero.

*The coefficient of pollution introduced by the cleaning, pickling and degreasing C_{pcd} is equal with 0.0005 kg of emissions.

*The coefficient of pollution introduced by the mechanical processing C_{pm} is of 0.0003 tons of emissions per ton of product.

*The coefficient of pollution introduced by products control and inspection noted with C_{cp} is of 0.010 kg of emissions.

*The coefficient of pollution C_{prrr} introduced for recovery, recycling and reconditioning noted with C_{prrr} is 0.5 kg of emissions.

*The auxiliary coefficient of pollution C_{pax} is zero, because it represents a fraction of the coefficient of pollution introduced by the semi-finished product C_{ps} which is also equal with zero

*The total coefficient of pollution C_{pt} is of 0.3 kilograms of emissions.

Third, for applying the “WIG re-melting weld toe” technique, we have the following results.

*The coefficient of pollution introduced by the semi-finished product C_{ps} is zero.

*The coefficient of pollution introduced by the raw materials supply C_{pa} is also zero.

*The coefficient of pollution introduced by the cleaning, pickling and degreasing C_{pcd} is equal with 0.0005 kg of emissions.

*The coefficient of pollution introduced by the mechanical processing C_{pm} is of 0.0001 tons of emissions per ton of product.

*The coefficient of pollution introduced by the products control and inspection noted with C_{cp} is kg of emissions.

*The coefficient of pollution C_{prrr} introduced for recovery, recycling and reconditioning noted with C_{prrr} is 0.5 kg of emissions.

*The auxiliary coefficient of pollution C_{pax} is zero, because it represents a fraction of the coefficient of pollution introduced by the semi-finished product C_{ps} which is also equal with zero

*The total coefficient of pollution C_{pt} is of 0.1135 kilograms of emissions.

The centralized results of the pollution coefficients obtained from the three variants of welding fabrication, application of the “weld toe grinding” technique and the “WIG re-melting weld toe” technique,” are presented in Table 12. The values of the pollution coefficients are expressed in kilograms of emissions per tons of product.

Table 12. Results for the coefficients of pollution for variants of welding fabrication.

Coefficient of Pollution/Fabrication Method	Welding Fabrication	The “Weld Toe Grinding” Technique	The “WIG Re-melting Weld toe” Technique
C_{ps} (kg of emissions)	12.820	0	0
C_{pa} (kg of emissions)	12.5	0	0
C_{pcd} (kg of emissions)	0.0005	0.0005	0.0005
C_{pm} (kg of emissions)	0.5	0.3	0.1
C_{cp} (kg of emissions)	0.015	0.010	0.013
C_{prrr} (kg of emissions)	0	0.5	0.5
C_{pax} (kg of emissions)	0.2565	0	0
C_{pt} (kg of emissions)	12.833	0.8105	0.6135

4. Conclusions

As we can observe from Figure 10 regardless of whether the rehabilitation techniques are applied or not, on the specimens D1, D4 and D7, all the fractures in the case of the static loads have occurred at a close range, between 57 to 59 kN. This means that none of those two rehabilitation techniques applied on the static tensile tests' specimens do not determine an increase in the breaking force, compared to the case where the rehabilitation technique does not apply. Based on this observation we can conclude that it is not justified to apply rehabilitation techniques to the welded structure statically stressed, made from an HSLA steel.

As can be seen in Figure 11, for the three sets of specimens from sample D, as follows: D2 and D3 without rehabilitation (green dot line curve), D5 and D6 with the "weld toe grinding" rehabilitation technique (broken green line) and D8 and D9 with the "WIG re-melting weld toe" rehabilitation technique (continuous green line), the durability curves are not asymptotic to the horizontal axis. All fatigue test specimens being manufactured and behaving like a welded structure, we can conclude that, practically, in the case of the fatigue stressed welded structures made from the HSLA steel, we cannot talk about the infinite fatigue resistance according to the classical Wohler curve. In the case of the fatigue test specimens due to the stress concentrators, we have a limited fatigue life time. This demonstrates that in the case of the fatigue stressed welded structures, in order to increase the fatigue lifetime, it is justified to apply the rehabilitation techniques. These rehabilitation techniques by reducing the stress concentrators both by grinding and WIG re-melting weld toe in the case of the welded structures, determine a decrease in the fatigue lifetime.

Also, from Figure 11, it is observed that for a certain value of the stress variation $\Delta\sigma$, the specimens D8 and D9 with the "WIG re-melting weld toe" rehabilitation technique applied, resist the greatest number of fatigue cycles until failure, the specimens without rehabilitation D2 and D3 resist the smallest number of the fatigue cycles until failure and the intermediate place is occupied by the specimens D5 and D6 with the "weld toe grinding" rehabilitation technique.

Based on the results centralized in Table 11, we can conclude that we have an increase of approximately 40% in the number of fatigue cycles up to fatigue failure in the case of "grinding weld toe" specimens, respectively with 195% in the case of "WIG re-melting weld toe" specimens, compared with the specimens without rehabilitation.

The metallographic analysis for all the specimens analysed, did not reveal structures outside the equilibrium, as we can observe from Figure 5. Also, as we can observe from Figure 7, from the variation of the micro-hardness from the axes I and II of all the analysed specimens, after the application of the rehabilitation techniques, no fragile structures in which the dangerous value of 350 Vickers units is exceeded, are obtained. This proves us that fatigue failures appeared only due to the stress concentrators and not because of some fragile metallographic structure.

Therefore, in the case of the HSLA welded structures fatigue stressed, it is justified to apply those two rehabilitation techniques "grinding weld toe" and "WIG re-melting weld toe", that have a beneficial influence in the case of the variable loads in the sense that they lead to increase the fatigue life time. But, the application of the rehabilitation techniques is not justified in the case of the statically loaded structures, to which these rehabilitation techniques do not bring any significant benefit.

As found in the calculation algorithm and in accordance with data from Table 11, the total coefficient of pollution has the smallest value for the "WIG re-melting weld toe" technique and the highest in the case of the welding fabrication of the product.

The general conclusion is that in the case of fatigue stressed structures such as bridges in welded construction, in order to increase the fatigue lifetime, it is justified to apply the "WIG re-melting weld toe" technique, this both from technically and from the environmental impact on the environment, point of view.

Author Contributions: All authors contributed equally to the research presented in this paper and to the preparation of the final manuscript.

Funding: This research received no external funding.

Acknowledgments: This research is part of an experiment elaborated by Claudiu Babis at the Politehnica University of Bucharest, Department of Welding and Materials Technology.

Conflicts of Interest: The authors declare no conflict of interest.

References

1. Cui, C.; Zhang, Q.; Bao, Y.; Kang, J.; Bu, Y. Fatigue performance and evaluation of welded joints in steel truss bridges. *J. Constr. Steel Res.* **2018**, *148*, 450–456. [[CrossRef](#)]
2. Cheng, B.; Ye, X.; Cao, X.; Mbako, D.D.; Cao, Y. Experimental study on fatigue failure of rib-to-deck welded connections in orthotropic steel bridge decks. *Int. J. Fatigue* **2017**, *103*, 157–167. [[CrossRef](#)]
3. Leander, J. Reliability evaluation of the Eurocode model for fatigue assessment of steel bridges. *J. Constr. Steel Res.* **2018**, *141*, 1–8. [[CrossRef](#)]
4. Berto, F. Fatigue Damage. *Metals* **2017**, *7*, 394. [[CrossRef](#)]
5. Yuan, H.; Zhang, W.; Castelluccio, G.M.; Kim, J.; Liu, Y. Microstructure-sensitive estimation of small fatigue crack growth in bridge steel welds. *Int. J. Fatigue* **2018**, *112*, 183–197. [[CrossRef](#)]
6. Bayraktar, E.; Xue, H.; Ayari, F.; Bathias, C. Torsional fatigue damage mechanisms in the very high cycle regime. *J. Arch. Mater. Sci. Eng.* **2010**, *43*, 77–86.
7. Chen, D.L.; Weiss, B.; Stickler, R.; Wang, Z.G. Re-considerations of fatigue crack closure effect. *Chin. J. Mater. Res.* **1995**, *9*, 162–179.
8. Chen, D.L.; Chaturvedi, M.C.; Goel, N.; Richards, N.L. Fatigue crack propagation behavior of X2095 Al-Li alloy. *Int. J. Fatigue* **1999**, *21*, 1079–1086. [[CrossRef](#)]
9. Hoh, H.J.; Pang, J.H.; Tsang, K.S. Stress intensity factors for fatigue analysis of weld toe cracks in a girth-welded pipe. *Int. J. Fatigue* **2016**, *87*, 279–287. [[CrossRef](#)]
10. Łagoda, T.; Bilous, P.; Blacha, Ł. Investigation on the effect of geometric and structural notch on the fatigue notch factor in steel welded joints. *Int. J. Fatigue* **2017**, *101*, 224–231. [[CrossRef](#)]
11. Xiao, Z.G.; Chen, T.; Zhao, X.L. Fatigue strength evaluation of transverse fillet welded joints subjected to bending loads. *Int. J. Fatigue* **2012**, *38*, 57–64. [[CrossRef](#)]
12. Wei, X.; Xiao, L.; Pei, S. Fatigue assessment and stress analysis of cope-hole details in welded joints of steel truss bridge. *Int. J. Fatigue* **2017**, *100*, 136–147. [[CrossRef](#)]
13. Shiozaki, T.; Yamaguchi, N.; Tamai, Y.; Hiramoto, J.; Ogawa, K. Effect of weld toe geometry on fatigue life of lap fillet welded ultra-high strength steel joints. *Int. J. Fatigue* **2018**, *116*, 409–420. [[CrossRef](#)]
14. Fricke, W.; Gao, L.; Paetzold, H. Fatigue assessment of local stresses at fillet welds around plate corners. *Int. J. Fatigue* **2017**, *101*, 169–176. [[CrossRef](#)]
15. Luo, P.; Zhang, Q.; Bao, Y.; Zhou, A. Fatigue evaluation of rib-to-deck welded joint using averaged strain energy density method. *Eng. Struct.* **2018**, *177*, 682–694. [[CrossRef](#)]
16. Cui, C.; Bu, Y.; Bao, Y.; Zhang, Q.; Ye, Z. Strain energy-based fatigue life evaluation of deck-to-rib welded joints in OSD considering combined effects of stochastic traffic load and welded residual stress. *J. Bridge Eng.* **2017**, *23*, 04017127. [[CrossRef](#)]
17. Cui, C.; Zhang, Q.; Bao, Y.; Bu, Y.; Ye, Z. Fatigue Damage Evaluation of Orthotropic Steel Deck Considering Weld Residual Stress Relaxation Based on Continuum Damage Mechanics. *J. Bridge Eng.* **2018**, *23*, 04018073. [[CrossRef](#)]
18. Zong, L.; Shi, G.; Wang, Y.Q.; Yan, J.B.; Ding, Y. Investigation on fatigue behaviour of load-carrying fillet welded joints based on mix-mode crack propagation analysis. *Arch. Civ. Mech. Eng.* **2017**, *17*, 677–686. [[CrossRef](#)]
19. Harati, E.; Karlsson, L.; Svensson, L.E.; Dalaei, K. The relative effects of residual stresses and weld toe geometry on fatigue life of weldments. *Int. J. Fatigue* **2015**, *77*, 160–165. [[CrossRef](#)]
20. Ngoula, D.T.; Beier, H.T.; Vormwald, M. Fatigue crack growth in cruciform welded joints: Influence of residual stresses and of the weld toe geometry. *Int. J. Fatigue* **2017**, *101*, 253–262. [[CrossRef](#)]
21. Ramalho, A.L.; Ferreira, J.A.; Branco, C.A. Fatigue behaviour of T welded joints rehabilitated by tungsten inert gas and plasma dressing. *Mater. Des.* **2011**, *32*, 4705–4713. [[CrossRef](#)]

22. Bayraktar, E.; Kaplan, D.; Schmidt, F.; Paqueton, H. GrumbachM State of art of impact tensile test (ITT): Its historical development as a simulated crash test of industrial materials and presentation of new “ductile/brittle” transition diagrams. *J. Mater. Process. Technol.* **2008**, *204*, 313–326. [[CrossRef](#)]
23. Iftime, E. Liability for Damage Caused by Dangerous Situations and Activities to the Environment. *Procedia Soc. Behav. Sci.* **2014**, *149*, 417–423. [[CrossRef](#)]
24. Iftime, E. Legal dimension of the responsibility for nuclear damage. *USV Ann. Econ. Public Admin.* **2013**, *13*, 236–244.
25. Maucher, H. Industry and the environment: The views of an industrialist. *Columbia J. World Bus.* **1993**, *28*, 6–10. [[CrossRef](#)]
26. Kessler, J.J.; Van Dorp, M. Structural adjustment and the environment: The need for an analytical methodology. *Ecol. Econ.* **1998**, *27*, 267–281. [[CrossRef](#)]
27. Sangwan, K.S.; Herrmann, C.; Egede, P.; Bhakar, V.; Singer, J. Life Cycle Assessment of Arc Welding and Gas Welding Processes. *Procedia CIRP* **2016**, *48*, 62–67. [[CrossRef](#)]



© 2018 by the authors. Licensee MDPI, Basel, Switzerland. This article is an open access article distributed under the terms and conditions of the Creative Commons Attribution (CC BY) license (<http://creativecommons.org/licenses/by/4.0/>).